

Effective Lagrangians and thermal resonances under extreme conditions

Andrea Vioque Rodríguez,^{a,*} Angel Gómez Nicola^a and Jacobo Ruiz de Elvira^a

^a*Departamento de Física Teórica and IPARCOS, Univ. Complutense, 28040 Madrid, Spain.*

E-mail: avioque@ucm.es, gomez@ucm.es, jacobore@ucm.es

We analyze various problems related to the physics of hadrons under extreme conditions of temperature and chemical potentials. On the one hand, we show that the thermal resonances $f_0(500)$ and $K_0^*(700)$, generated in the framework of Unitarized Chiral Perturbation Theory $\pi\pi$ and $K\pi$ scattering at finite temperature, play an essential role concerning chiral and $U(1)_A$ restoration. On the other hand, a low-energy effective Lagrangian has been constructed within ChPT at non-zero chemical potential, which we discuss here for an axial chemical potential.

*10th International Conference on Quarks and Nuclear Physics
8-12 July, 2024
Barcelona, Spain*

*Speaker

1. Introduction

The main goal of this talk is to study the nature of the chiral transition and its connection to the $U_A(1)$ symmetry restoration using effective theories. Chiral symmetry can be restored by external effects such as temperature. At $\mu_B = 0$, lattice simulations have quite firmly established that the chiral transition is a crossover at $T_c \simeq 155$ MeV for $2 + 1$ flavors and physical quark masses [1, 2], usually identified as the peak position of the scalar susceptibility. The subtracted quark condensate and chiral susceptibility are the key observables to study the chiral transition.

Another important problem, still under investigation, is whether $U_A(1)$ restoration occurs close to the chiral transition. While for $N_f = 2 + 1$ lattice simulations with physical quark masses, the $U_A(1)$ symmetry remains significantly broken at the chiral transition [3], $N_f = 2$ analyses near the light chiral limit indicate compatibility between chiral and $U_A(1)$ restoration [4, 5].

2. Scattering and resonances within finite temperature Unitarized ChPT

A central aspect of our analysis is the study of light thermal resonances, generated through the unitarization of scattering amplitudes at finite temperature [6]. Due to interactions with particles in the thermal environment, resonances can experience significant changes in their spectral properties. This is studied by examining the second Riemann sheet pole of the unitarized scattering amplitudes, computed within Chiral Perturbation Theory (ChPT) at finite temperature [7, 8].

At $T = 0$ and within ChPT, a two-body $a + b \rightarrow a + b$ elastic partial-wave scattering amplitude reads $t(s) = t_2(s) + t_4(s) + \dots$, where t_2 is the tree-level contribution coming from the $\mathcal{O}(p^2)$ Lagrangian and t_4 containing one-loop diagrams from the second-order ChPT Lagrangian as well as tree-level terms from the fourth-order one proportional to the low-energy constants (LECs). The amplitude is extended to finite temperature through the replacement $t_4(s) \rightarrow t_4(s; T)$ and then unitarized using the Inverse Amplitude Method (IAM), resulting in

$$t_{IAM}(s, T) = \frac{t_2(s)^2}{t_2(s) - t_4(s, T)}, \quad (1)$$

which satisfies exact thermal elastic unitarity [9]

$$\text{Im } t_{IAM}(s, T) = \begin{cases} \sigma_{ab}^T(s) [t_{IAM}(s, T)]^2, & s \geq (M_a + M_b)^2, \\ \tilde{\sigma}_{ab}^T(s) [t_{IAM}(s, T)]^2, & 0 \leq s \leq (M_a - M_b)^2, \end{cases} \quad (2)$$

where M_a and M_b are the masses of particle a and b , respectively, and $\sigma_{ab}^T(s)$ and $\tilde{\sigma}_{ab}^T(s)$ read

$$\sigma_{ab}^T(s) = \sigma_{ab}(s) \left[1 + n_B \left(\frac{s + \Delta_{ab}}{2\sqrt{s}} \right) + n_B \left(\frac{s - \Delta_{ab}}{2\sqrt{s}} \right) \right], \quad (3)$$

$$\tilde{\sigma}_{ab}^T(s) = \sigma_{ab}(s) \left[n_B \left(\frac{\Delta_{ab} - s}{2\sqrt{s}} \right) - n_B \left(\frac{s + \Delta_{ab}}{2\sqrt{s}} \right) \right], \quad (4)$$

with $\Delta_{ab} = M_a^2 - M_b^2$ and n_B the Bose-Einstein distribution function.

As in the $T = 0$ case, one has the standard unitary cut starting from the two-particle scattering threshold. At finite temperature and for $M_a \neq M_b$, a new cut appears, the so-called Landau cut.

These cuts can be explained by the scattering of particles in the thermal bath. In other words, the statistical Bose-Einstein weights appearing in the thermal phase space factors (3)-(4) can be interpreted considering the stimulated production processes and the absorption by the thermal bath.

In [9], we have computed the πK elastic scattering amplitude and studied the thermal trajectories of the $K_0^*(700)$ and $K^*(892)$ resonances. In Figure 1, we can see that the $K_0^*(700)$ mass shows a decreasing trend at larger temperatures while its width increases at low temperatures but decreases at larger T values. The $K^*(892)$ pole has a softer temperature dependence, consistent with a smoother medium dependence than for the $\rho(770)$.

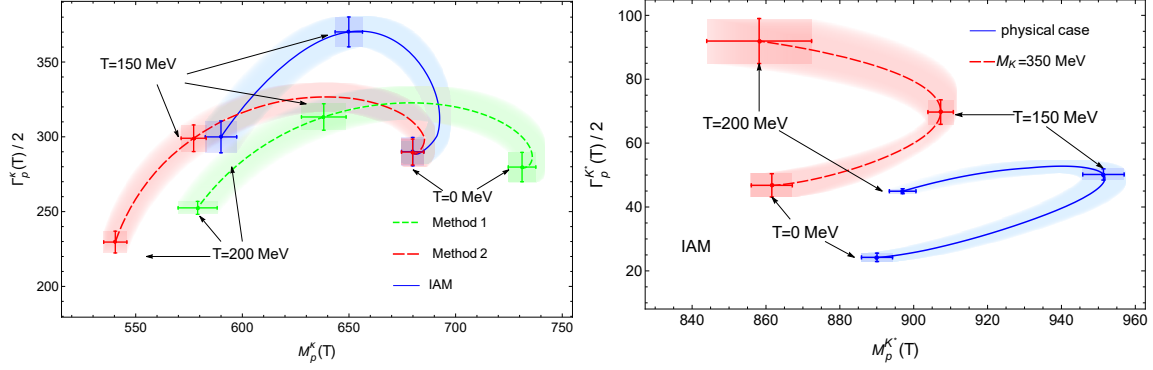


Figure 1: Thermal dependence of the $K_0^*(700)$ (left) and $K^*(892)$ (right) poles. The pole is parameterized as customary as $\sqrt{s_p(T)} = M_p(T) - i\Gamma_p(T)/2$. The error bands correspond to the uncertainties in the LECs.

3. Scalar susceptibilities and light thermal resonances

Another important outcome is the analysis of the scalar susceptibility χ_S . As described in [10, 11], it can be saturated by the lightest thermal resonance $f_0(500)$

$$\chi_S^U(T) = \chi_S^{ChPT}(0) \frac{M_S^2(0)}{M_S^2(T)}, \quad (5)$$

where $M_S^2(T) = \text{Re } s_p(T)$ is its thermal mass. Using the $f_0(500)$ thermal pole from the unitarized $\pi\pi$ scattering amplitude obtained at finite temperature [6], this approach provides a robust description of the scalar susceptibility near the chiral transition. As shown in Figure 2, the saturated susceptibility reproduces the crossover maximum and is compatible with lattice results below and near the critical temperature, which highlights the close relationship between resonance dynamics and the behavior of QCD near the critical temperature.

As an alternative sector to analyze chiral and $U_A(1)$ restoration, we have studied the isospin 1/2 channel. The quark bilinears of the kaon and κ mesons are related by both a chiral $O(4)$ and a $U_A(1)$ transformations, and hence, $O(4) \times U_A(1)$ restoration can be studied from $K - \kappa$ degeneration using the $I = 1/2$ Ward Identities (WIs) [13, 14]

$$\chi_P^K(T) = \frac{[\langle \bar{q}q \rangle_l + 2\langle \bar{s}s \rangle]}{m_s - m_l}, \quad \chi_S^K(T) = -\frac{[\langle \bar{q}q \rangle_l - 2\langle \bar{s}s \rangle]}{m_s + m_l}. \quad (6)$$

Taking the difference between the two WIs, it follows that $K - \kappa$ degeneration is controlled by the subtracted quark condensate, i.e., $\chi_P^K - \chi_S^K \propto \Delta_{l,s}$, available in the lattice [2]. In the $m_s \gg m_l$ two-flavor limit, $\Delta_{l,s}$ is proportional to the light-quark condensate $\langle \bar{q}q \rangle_l$, implying $K - \kappa$ degeneration

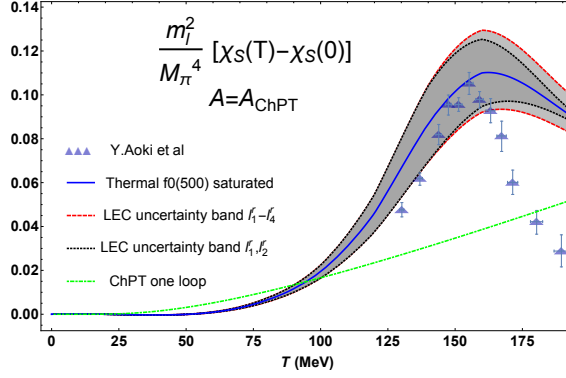


Figure 2: Saturated susceptibility including the LEC uncertainties given in [12]. Lattice points are from [1].

at the critical temperature in the exact chiral limit. In the physical case, $\Delta_{l,s}$ shows an asymptotic vanishing behavior only at larger temperatures, so the effective $O(4) \times U_A(1)$ restoration occurs only above T_c . Hence, m_l/m_s is a relevant parameter regarding the behavior of the $K - \kappa$ susceptibility difference, and this channel helps to understand the difference between the $N_f = 2 + 1$ and $N_f = 2$ lattice results.

In the $I = 1/2$ channel, it is expected that the contribution of the $K_0^*(700)$ to χ_S^K will be the most dominant because it is the lightest scalar state in this channel. Therefore, analogous to how the scalar susceptibility χ_S was saturated with the $f_0(500)$, we construct a unitarized susceptibility χ_S^K by saturating it with the thermal $K_0^*(700)$ pole. For the unitarized χ_S^K , we get the same behavior as for the reconstructed susceptibility from lattice results using the light- and strange-quark condensates. In Figure 3, we can see the peak of the χ_S^K scalar susceptibility at a temperature above the chiral critical temperature. We can also note that near the light-chiral limit ($M_\pi = 20$ MeV) the growth of the curve below the peak is more pronounced and compatible with a flattening above the peak, which seems to indicate $K - \kappa$ degeneration at lower temperatures. Close to the $SU(3)$ limit ($M_K = 350$ MeV), the peak displaces towards T_c and grows, consistent with the degeneration of χ_S^K with χ_S .

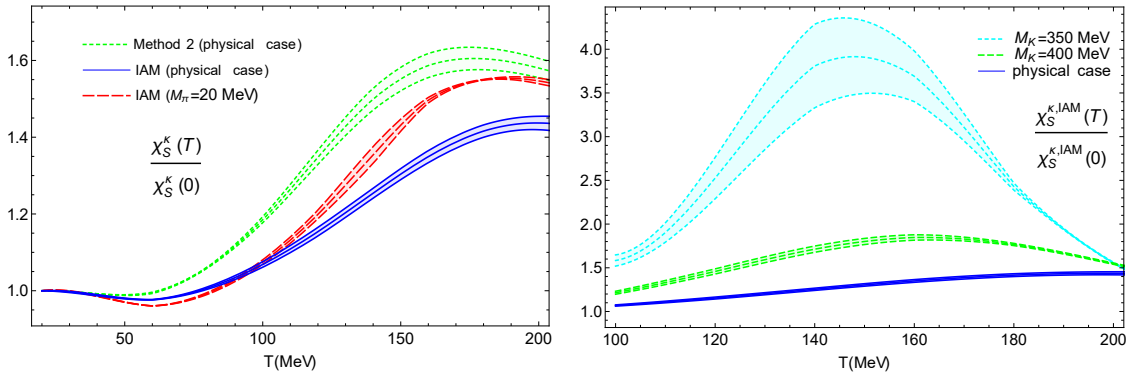


Figure 3: Temperature dependence of the unitarized κ susceptibility for physical masses and the light chiral limit (left) and for M_K closer to the $SU(3)$ limit (right).

4. Pion scattering and critical temperature at nonzero chiral imbalance

Finally, we have explored the evolution of chiral restoration for nonzero chiral imbalance chemical potential μ_5 . For this purpose, we have constructed the most general effective Lagrangian for a nonzero axial chemical potential μ_5 [15] through the so-called external source method. This Lagrangian includes different types of terms coming from the covariant derivatives and explicit source terms. While the μ_5 dependence of the second-order Lagrangian is a constant term, the fourth-order chiral Lagrangian is modified in the following way

$$\mathcal{L}_4(\mu_5) = \mathcal{L}_4(\mu_5 = 0) + \kappa_1 \mu_5^2 \text{tr}(\partial^\mu U^\dagger \partial_\mu U) + \kappa_2 \mu_5^2 \text{tr}(\partial_0 U^\dagger \partial^0 U) + \kappa_3 \mu_5^2 \text{tr}(\chi^\dagger U + U^\dagger \chi) + \kappa_4 \mu_5^4. \quad (7)$$

From the energy density obtained within the above equation (7), we derive the quark condensate. This quantity can be used to extract some information about the κ_i LECs involved from the critical temperature determined as the value for which the quark condensate vanishes. At NNLO, the light quark condensate normalized to its zero temperature value depends only on the combinations $\kappa_a = 2\kappa_1 - \kappa_2$ and $\kappa_b = \kappa_1 + \kappa_2 - \kappa_3$. On the other hand, the chiral critical temperature can be defined as the temperature at which the scalar susceptibility has a maximum, so we can calculate this one from the saturated approach mentioned in the previous section. To obtain the μ_5 dependence of the saturated susceptibility, we have calculated the μ_5 corrections to the unitarized $\pi\pi$ elastic scattering amplitude within the ChPT framework at finite temperature [16]. The μ_5 dependence of the $IJ = 00$ perturbative ChPT partial wave depends on two different κ_i combinations: $\kappa'_1 = 6\kappa_1 + 5\kappa_2$ and $\kappa'_2 = -8\kappa_1 - 4\kappa_2 + 5\kappa_3$.

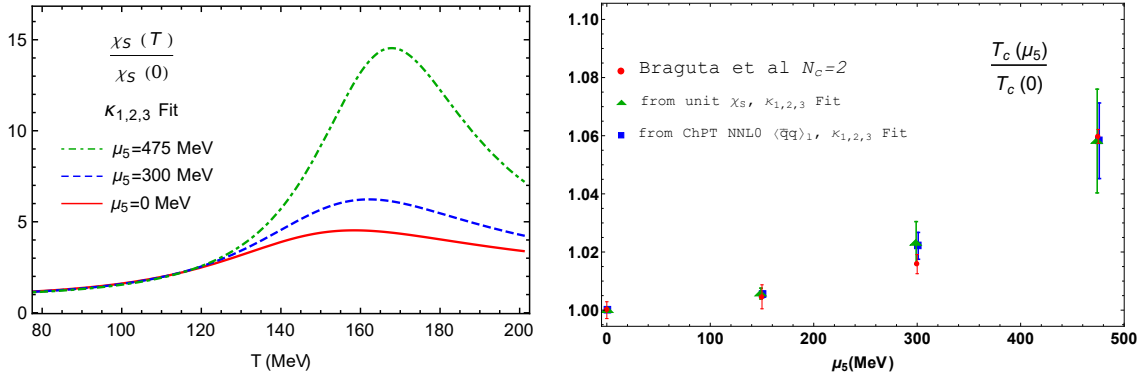


Figure 4: Left: Right: Combined fit of $T_c(5)/T_c(0)$ determined from the NNLO ChPT quark condensate, the saturated susceptibility, and the topological susceptibility. We also show the lattice results from [17].

We have carried out a combined fit with $\kappa_{1,2,3}$ as fit parameters where the fitted observables are the critical temperature with both methods mentioned, namely, the ChPT condensate and the scalar susceptibility, and the topological susceptibility analyzed in [15]. The result of the fit is $\kappa_1 = 9.4^{+1.1}_{-1.3}$, $\kappa_2 = -4.5^{+1.5}_{-1.4}$ and $\kappa_3 = 3.6^{+9.1}_{-8.7}$ where the uncertainties corresponds to the 95% confidence level. Figure 4 shows the saturated susceptibility and the critical temperature plotted with the κ_i set corresponding to our fit. As we can see, lattice points are compatible with both T_c determinations, confirming the growing behavior of the critical temperature when chiral imbalance is increased.

5. Conclusions

We have demonstrated the importance of the $f_0(500)$ and κ thermal resonances in chiral and $U_A(1)$ symmetry restoration. Our results show that the mass and the width of these resonances undergo significant shifts with increasing temperature, consistent with the expected behavior near the chiral transition. In addition, the χ_S and χ_S^K saturated susceptibilities reveal a behavior consistent with the lattice results. Finally, we have analyzed chiral restoration in the presence of chiral imbalance and found that the chiral critical temperature increases with μ_5 , corroborating lattice studies.

Acknowledgments

Work supported by the Ministerio de Ciencia e Innovación, research contract PID2022-136510NB-C31, the European Union Horizon 2020 program under grant agreement No 824093, and the Ramón y Cajal program (RYC2019-027605-I) of the Spanish MINECO.

References

- [1] Y. Aoki *et al.* JHEP **06** (2009), 088.
- [2] A. Bazavov *et al.* Phys. Rev. D **85** (2012), 054503.
- [3] M. I. Buchoff *et al.*, Phys. Rev. D **89** (2014) no.5, 054514.
- [4] B. B. Brandt *et al.*, JHEP **12** (2016), 158.
- [5] A. Tomiya *et al.*, Phys. Rev. D **96** (2017) no.3, 034509.
- [6] A. Dobado *et al.*, Phys. Rev. C **66** (2002), 055201.
- [7] A. Gomez Nicola *et al.*, Phys. Rev. D **87** (2013), 016001, Phys. Rev. D **82** (2010), 074012.
- [8] A. Gómez Nicola, J. Ruiz De Elvira and A. Vioque-Rodríguez, JHEP **11** (2019), 086.
- [9] A. Gómez Nicola, J. Ruiz de Elvira and A. Vioque-Rodríguez, JHEP **08** (2023), 148.
- [10] A. Gomez Nicola, J. Ruiz de Elvira and R. Torres Andres, Phys. Rev. D **88** (2013), 076007.
- [11] S. Ferreres-Solé *et al.*, Phys. Rev. D **99** (2019) no.3, 036018.
- [12] C. Hanhart, J. R. Pelaez and G. Rios, Phys. Rev. Lett. **100** (2008), 152001.
- [13] A. Gómez Nicola and J. Ruiz de Elvira, JHEP **03** (2016), 186, Phys. Rev. D **97** (2018) no.7, 074016, Phys. Rev. D **98** (2018) no.1, 014020.
- [14] A. Gómez Nicola *et al.*, Eur. Phys. J. C **81** (2021) no.7, 637.
- [15] D. Espriu, A. Gómez Nicola and A. Vioque-Rodríguez, JHEP **06** (2020), 062.
- [16] A. Gómez Nicola *et al.*, Phys. Rev. D **109** (2024) no.3, 034011.
- [17] V. V. Braguta *et al.* JHEP **06** (2015), 094.